Hormones and Behavior 74 (2015) 149–156

Contents lists available at ScienceDirect

Hormones and Behavior

journal homepage: www.elsevier.com/locate/yhbeh

Estradiol rapidly modulates spinogenesis in hippocampal dentate gyrus: Involvement of kinase networks

Yasushi Hojo [a,b], Arisa Munetomo [a], Hideo Mukai [a,b], Muneki Ikeda [a], Rei Sato [a], Yusuke Hatanaka [a], Gen Murakami [a,b], Yoshimasa Komatsuzaki [a], Tetsuya Kimoto [a], Suguru Kawato [a,b,c,*]

[a] Department of Biophysics and Life Sciences, Graduate School of Arts and Sciences, University of Tokyo, Komaba 3-8-1, Meguro, Tokyo 153-8902, Japan
[b] Bioinformatics Project of Japan Science and Technology Agency, University of Tokyo, Japan
[c] Department of Urology, Juntendo University, Graduate School of Medicine, Tokyo 113-8431, Japan

ARTICLE INFO

Available online 27 June 2015

Keywords:
17β-Estradiol
Estrogen receptor
Dentate gyrus
Hippocampus
Spine
Spinogenesis
Synapse

ABSTRACT

This article is part of a Special Issue "Estradiol and cognition".

Estradiol (E2) is locally synthesized within the hippocampus and the gonads. Rapid modulation of hippocampal synaptic plasticity by E2 is essential for synaptic regulation. The molecular mechanisms of modulation through the synaptic estrogen receptor (ER) and its downstream signaling, however, are largely unknown in the dentate gyrus (DG). We investigated the E2-induced modulation of dendritic spines in male adult rat hippocampal slices by imaging Lucifer Yellow-injected DG granule cells. Treatments with 1 nM E2 increased the density of spines by approximately 1.4-fold within 2 h. Spine head diameter analysis showed that the density of middle-head spines (0.4–0.5 μm) was significantly increased. The E2-induced spine density increase was suppressed by blocking Erk MAPK, PKA, PKC and LIMK. These suppressive effects by kinase inhibitors are not non-specific ones because the GSK-3β antagonist did not inhibit E2-induced spine increase. The ER antagonist ICI 182,780 also blocked the E2-induced spine increase. Taken together, these results suggest that E2 rapidly increases the density of spines through kinase networks that are driven by synaptic ER.

Introduction

The hippocampus is heavily involved in learning and memory processes. Findings that estrogen and androgen are synthesized in the adult male/female hippocampus have opened a new field of study regarding estrogen function as it relates to the regulation of daily memory formation (Kimoto et al., 2001; Kawato et al., 2002, 2003; Hojo et al., 2004, 2008; Kretz et al., 2004; Mukai et al., 2006a, 2010; Murakami et al., 2006a; Munetsuna et al., 2009).

The level of adult hippocampal 17β-estradiol (E2) is higher (~8 nM in male, 0.5–4 nM in female) than that of plasma E2 (0.02–0.1 nM), as determined by mass spectrometric analysis (Hojo et al., 2009, 2014; Kato et al., 2013).

Hippocampal glutamatergic neurons express estrogen receptors (ERs). Both forms, ERα and ERβ, are located not only in the cytoplasm and the nuclei but also within dendritic spines (Milner et al., 2005; Mukai et al., 2007, 2010; Hojo et al., 2008; Murakami et al., 2014). Therefore, E2 could produce rapid non-genomic effects (occurring within 2 h of exposure) through synaptic ERs. Of course, chronic and genomic effects (occurring over 1–5 days) can also occur through nuclear/cytoplasmic ERα/ERβ.

We should seriously consider the modulatory actions of hippocampus-derived E2 (Tsurugizawa et al., 2005; Mukai et al., 2007, 2010; Tanaka and Sokabe, 2012; Pettorossi et al., 2013; Luine, 2014; Hasegawa et al., 2015) in addition to the functions of gonadal E2 (Gould et al., 1990; Woolley et al., 1990; Woolley and McEwen, 1992; Leranth et al., 2003). Accumulating evidence suggests that E2 has acute modulatory effects on spinogenesis, long-term potentiation (LTP) and long-term depression (LTD) in the CA1 and CA3 regions. In previous studies, we showed that 2 h incubation in 1 nM E2 increased dendritic spine density in the CA1 stratum radiatum and decreased the density of dendritic thorns in the CA3 stratum lucidum. From mechanistic analyses, these rapid E2 effects have been shown to be mediated by various kinase networks, including Erk MAPK, PI3K, PKA, PKC and LIMK (Tsurugizawa et al., 2005; Murakami et al., 2006b; Ishii et al., 2007; Hojo et al., 2008; Ogiue-Ikeda et al., 2008; Hasegawa et al., 2015).

The dentate gyrus (DG) receives excitatory inputs from the lateral and medial entorhinal cortex through the perforant path into the molecular layer (Thomas et al., 1994; Dolorfo and Amaral, 1998). The perforant path terminates in synaptic contacts with dendritic spines of granule neurons. The DG plays an essential role in several cognitive functions, including pattern separation (McHugh et al., 2007; Aimone

* Corresponding author at: Department of Biophysics and Life Sciences, Graduate School of Arts and Sciences, University of Tokyo, Komaba 3-8-1, Meguro, Tokyo 153-8902, Japan.
E-mail address: kawato@bio.c.u-tokyo.ac.jp (S. Kawato).

http://dx.doi.org/10.1016/j.yhbeh.2015.06.008
0018-506X/

et al., 2011) and the formation of contextual fear-conditioned memories (Liu et al., 2014). The DG has also been studied extensively as a region of adult neurogenesis (Kuiper et al., 1997; Perez-Martin et al., 2003a; Olariu et al., 2005; Tanapat et al., 2005). LTP in the DG has also been investigated (Trommald et al., 1996), and it has been found that this phenomenon correlates with spatial pattern separation (Clelland et al., 2009; Nakashiba et al., 2012).

However, only a few studies have been reported concerning the effects of estrogen on spinogenesis in the DG (Miranda et al., 1999). We therefore investigated whether E2 can rapidly increase the presence of spines on granule neurons in the adult male hippocampal DG region. Furthermore, we investigated whether multiple kinases might be involved in E2 signaling.

Materials and methods

Animals

Twelve-week-old adult male Wistar rats were purchased from Tokyo Experimental Animal Supply. All experimental procedures used for this research were approved by the Committee for Animal Research of Univ. of Tokyo.

Chemicals

Lucifer Yellow and LY294002 were purchased from Sigma (USA). Chelerythrine, H-89, GSK-3β Inhibitor 8 (I8), and LIMK inhibitor (LIMKi) were purchased from Calbiochem (USA). 17β-estradiol (E2), U0126 and ICI 182,780 (ICI) were purchased from Wako Pure Chemical Industries (Japan).

Imaging and analysis of dendritic spine density and morphology

Hippocampal slice preparation and current injection of Lucifer Yellow

Male rats aged 12 weeks were deeply anesthetized and decapitated. The brains were removed and placed in artificial cerebrospinal fluid (ACSF) at 4 °C. ACSF consisted of (mM) 124 NaCl, 5.0 KCl, 1.25 NaH_2PO_4, 2.0 $MgSO_4$, 2.0 $CaCl_2$, 22 $NaHCO_3$, and 10 glucose and was equilibrated with 95% O_2/5% CO_2. The hippocampus was dissected, and 300-μm slices transverse to the long axis from the middle third of the hippocampus were cut using a vibratome (Dosaka, Japan). These 'fresh' hippocampal slices were transferred into an incubating chamber containing ACSF held at 25 °C and kept there for 2 h for slice recovery. The resulting 'acute' slices were then incubated in 0.1–10 nM E2 together with ER antagonist (ICI 182,780) or inhibitors of protein kinases. All steroids, antagonist and inhibitors were diluted with 1/1000 dimethylsulfoxide (DMSO) in ASCF. Slices were then fixed with 4% paraformaldehyde in PBS at 4 °C overnight. Neurons within slices were visualized by injecting the tissue with Lucifer Yellow (Molecular Probes, USA) and placing it in a Nikon E600FN microscope (Japan) equipped with a C2400-79H infrared camera (Hamamatsu Photonics, Japan) and a 40× water immersion lens (Nikon, Japan). Dye injection was performed using a glass electrode filled with 5% Lucifer Yellow for 15 min, using Axopatch 200B (Axon Instruments, USA). Approximately five neurons within a depth of 100 μm from the surface of a slice were injected with Lucifer Yellow (Duan et al., 2003).

Confocal laser microscopy and morphological analysis

Imaging was performed by taking sequential z-series scans with a confocal laser scanning microscope (LSM5; Carl Zeiss, Germany), at high zoom (3.0×) with a 63× water immersion lens, NA 1.2. For Lucifer Yellow, the excitation and emission wavelengths were 488 nm and 515 nm, respectively. For analysis of spines, three-dimensional images were reconstructed from approximately 40 sequential z-series sections taken 0.45 μm apart with a 63× water immersion lens, NA 1.2. The applied zoom factor (3.0×) yielded 23 pixels per μm. The z-axis resolution was approximately 0.71 μm per section. The confocal lateral resolution was approximately 0.26 μm per pixel. Our resolution limits were considered to be sufficient to allow for the determination of spine density. Confocal images were then deconvolved using AutoDeblur software (AutoQuant, USA).

The density of spines and spine head diameters were analyzed using Spiso-3D (automated software that calculates the geometrical parameters of spines), which was developed as part of the Kawato group's Bioinformatics Project (Mukai et al., 2011). Spiso-3D has functionality that is equivalent to Neurolucida (MicroBrightField, USA); furthermore, Spiso-3D considerably reduces the number of human errors and the amount of experimenter labor required for analysis. Each dendrite was analyzed separately. Spine density was calculated from the numbers of spines along dendrites having a total length of 50 to 100 μm. These dendrites were present within the outer molecular layer, between 50 and 150 μm from the soma. Spine shapes were classified into three categories, as follows: (1) Small-head spines, whose head diameters are between 0.2 and 0.4 μm. (2) Middle-head spines, which have spine heads measuring 0.4–0.5 μm. (3) Large-head spines, whose head diameters are between 0.5 and 1.0 μm. These three categories were useful for distinguishing between responses to different kinase inhibitor applications. Because the majority of spines observed (>95%) had a distinct head and neck and because stubby spines and filopodium did not considerably contribute to the overall changes, we only analyzed spines with a distinct head.

Post-embedding immunogold method for electron microscopy

Immunoelectron microscopy analysis was performed as described elsewhere (Mukai et al., 2007). Rat hippocampus was coronally sliced at 4 °C using a vibratome. Freeze substitution and low-temperature embedding of the specimens were performed as described previously (Adams et al., 2002). The samples were immersed in uranyl acetate in anhydrous methanol (−90 °C). They were then infiltrated with Lowicryl HM20 resin (Electron Microscopy Sciences, USA), and polymerization was performed using ultraviolet light. Ultrathin sections were prepared using a Reichert-Jung ultramicrotome. For immunolabeling, sections were incubated overnight in either RC-19 (Mukai et al., 2007), purified primary antibody for ERα (diluted to 1/1000), or anti-human cytochrome P450arom IgG (Hojo et al., 2004) (diluted to 1/500), followed by incubation with secondary gold-tagged (10 nm) Fab fragments in Tris-buffered saline (TBS). Sections were counterstained with 1% uranyl acetate and viewed on a JEOL 1200EX electron microscope (Japan). Images were captured using a CCD camera (Advanced Microscopy Techniques, USA).

Statistical analysis

The significance of the effects of incubating in E2 or other drugs was examined via statistical analysis using Tukey–Kramer post-hoc multiple comparisons test when one-way ANOVA tests yielded $P < 0.05$.

Results

We investigated the effect of E2 on modulation of the dendritic spine density in the hippocampus dentate gyrus molecular layer. Lucifer Yellow-injected neurons in hippocampal slices from 12-week-old male rats were imaged using confocal laser scanning microscopy and analyzed using Spiso-3D software (Fig. 1A, B). Spines within 50 μm to 150 μm from the soma where the perforant path from entorhinal cortex attached were studied (Fig. 1C).

Estrogen-related increase in spine density in DG molecular layer

The level of E2 in control slices was below 0.5 nM because E2 was leaked to the outer medium during the 2-h recovery incubation in

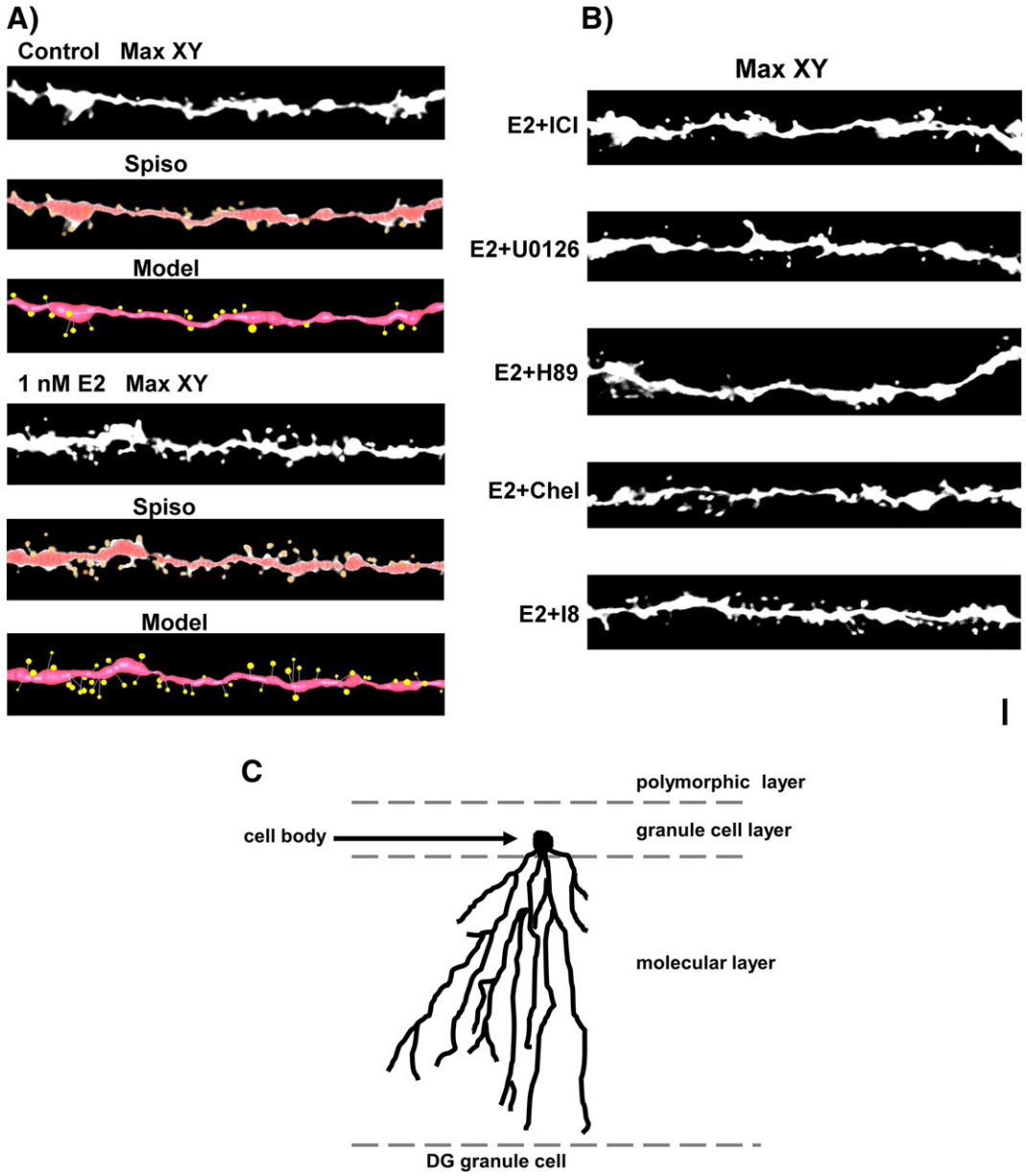

Fig. 1. E2-induced spine increase of DG granule cells in hippocampal slices. (A) Dendritic spines without drug treatment (control), and with 1 nM E2 treatment for 2 h. Bar 2 μm. Upper images (Max XY) show maximal intensity projections onto the XY plane from z-series confocal micrographs. Spines along the dendrites of hippocampal DG granule cells are visible. Middle images (Spiso) show a traced dendrite (connected series of red circles) and spines (yellow circles) superimposed on the image by Spiso-3D. Lower images (Model) show a 3D model of the traced dendrite and spines. (B) Max XY images of dendritic spines after a 2-h treatment in ACSF with 1 nM E2 and ICI (E2 + ICI), with 1 nM E2 and U0126 (E2 + U0126), with 1 nM E2 and H-89 (E2 + H89), with 1 nM E2 and Chelerythrine (E2 + Chel), and with 1 nM E2 and Inhibitor 8 (E2 + I8). (C) Traced image of a whole granule neuron in DG. Spines on the dendrites in the outer molecular layer were analyzed in the current study.

ACSF (Hojo et al., 2011; Ooishi et al., 2012a, 2012b). Following a 2-h treatment with E2, treated dendrites had significantly more spines than control dendrites (where no E2 was added). Dose dependence was examined by treating slices with 0.1, 1 and 10 nM E2 for 2 h. The increase produced by E2 on the total spine density was significant at 1 nM (1.15 spines/μm) and 10 nM (1.15 spines/μm), whereas the spine density at 0.1 nM (0.93 spines/μm) showed no marked increase from the control (0.81 spines/μm) (Fig. 2A). Note that 1 nM is close to the lowest concentration of E2 found in freshly prepared hippocampus (which typically contains 2–13 nM E2) but is much higher than the male plasma E2 level (~0.01 nM) (Hojo et al., 2009).

Blocking ERα/ERβ with 1 μM ICI, an inhibitor of ER, completely abolished the effect of E2 on the spine density (0.86 spines/μm were measured) (Fig. 2A).

Subpopulation analysis of spine head diameter

The morphological changes in spine head diameter induced by 2-h treatment were assessed. Although the effects of E2 dose-dependent treatment on total spine density were indistinguishable in cases where the E2 concentration caused a significant change, closer examination of spine head diameters revealed a difference in the distribution of spine head diameters between 1 nM E2 and 10 nM E2 treatments (Fig. 2B). To distinguish different responses in spine subpopulations, spines were classified into 3 categories according to their head diameters: small-head spines, middle-head spines, and large-head spines (Fig. 2C). In control slices (with no E2), the spine density was 0.38 spines/μm for small-head spines, 0.28 spines/μm for middle-head spines, and 0.14 spines/μm for large-head spines. Upon treatment with 1 nM E2, the density of middle-head spines increased significantly,

whereas the densities of small- and large-head spines were not significantly altered. Upon treatment with 10 nM E2, the densities of middle- and large-head spines increased significantly, whereas the density of small-head spines was not significantly different. The increase of middle-head spines elicited by treatment with 1 nM E2 was completely abolished by co-application of 1 nM E2 with ICI.

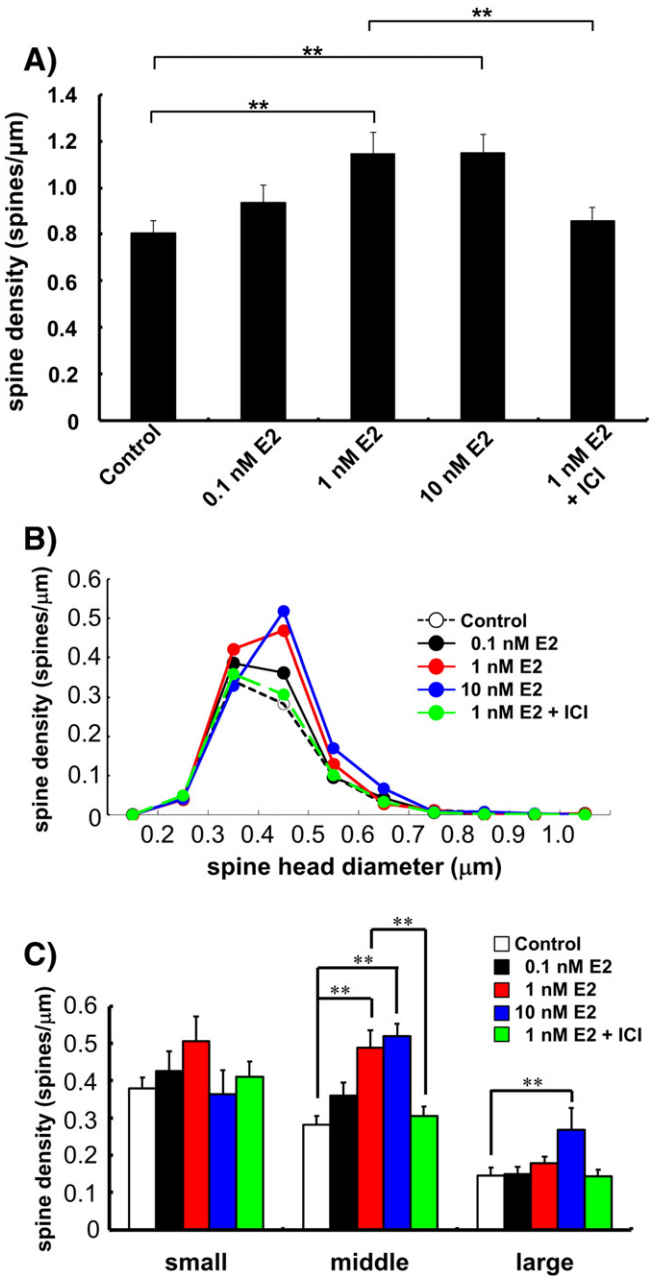

Fig. 2. Change in the density and morphology of spines by E2 and ICI. (A) Dose dependence of E2 effect on total spine density. After a 2-h treatment in ACSF without E2 (control), with 0.1 nM E2, 1 nM E2, and 10 nM E2. The effect of an antagonist for estrogen receptors, ICI (1 μM), is also shown (1 nM E2 + ICI). (B) Histogram of spine head diameters after a 2-h treatment in ACSF without E2 (control, dashed line), with 0.1 nM E2 (black line), 1 nM E2 (red line), 10 nM E2 (blue line), and with 1 nM E2 and ICI (green line). (C) Densities of three subtypes of spines. From left to right, small-head spines (small), middle-head spines (middle), and large-head spines (large). A 2-h treatment in ACSF without drugs (control, open column), with 0.1 nM E2 (black column), with 1 nM E2 (red column), with 10 nM E2 (blue column), with 1 nM E2 and ICI (green column). Vertical axis is the average number of spines per 1 μm of dendrite. Results are represented as the mean ± SEM. Significance is defined as *: $P < 0.05$, **: $P < 0.01$ versus control or 1 nM E2. For each drug treatment, we investigated 3 rats, 6 slices, 14 neurons, 28 dendrites and 1300–1900 spines. For the control, we used 5 rats, 8 slices, 16 neurons, 31 dendrites and approx. 1700 spines.

Signaling pathways depending on protein kinases

Next, we investigated intracellular signaling pathways of several kinases potentially involved in the estrogen-induced spine increase by using selective inhibitors for kinases (Fig. 3A). Blocking Erk MAPK by application of 25 μM U0126 abolished the E2-related increase of total spine density. Application of 10 μM Chelerythrine, a non-selective PKC subfamily inhibitor, also prevented the increase in spine density after E2 treatment, as did the application of 10 μM H-89, an inhibitor of PKA, and the application of 10 μM LIMKi, an inhibitor of LIMK. However, selective inhibition of GSK-3β (by 50 μM Inhibitor 8) did not suppress the effect of E2.

To describe the complex effects of kinases precisely, the changes in spine head diameter distribution were analyzed for particular kinases (Fig. 3B, C). It was found that the increase of middle-head spines by treatment with 1 nM E2 was suppressed by co-application of E2 with U0126, E2 with H-89, or E2 with Chelerythrine. Such suppression was not observed for application of E2 with I8. No effects were observed upon treatment with inhibitors only (Fig. 3D). Therefore, several kinases were shown to play an essential role in spinogenesis by rapid effects of E2.

Ultrastructural analysis for synaptic localization of ERα and cytochrome P450arom

To understand the localization of rapid modulation of spinogenesis in DG glutamatergic neurons by the activation of ERα, knowledge of the subcellular and particularly the synaptic localizations of ERα in glutamatergic neurons is essential. The synaptic localization of ERα was visualized via ultrastructural investigations using RC-19 (1/1000) (ERα specific purified IgG) (Mukai et al., 2007). Immunoelectron microscopy analysis using post-embedded immunogold was performed to determine the localization of ERα-immunoreactivity in DG granule cells of adult male rats. ERα was localized in both the axon terminals and dendritic spines (Fig. 4A). In the postsynaptic processes, gold particles were distributed within the cytoplasm of the spine head. We examined over 50 images in our search for immunogold-labeled ERα proteins. Each image contained several synapses, among which at least one expressed ERα particles. We also observed some synapses in one image that did not express ERα particles. Consequently, we observed that approx. 25–30% of synapses expressed ERα particles. We also investigated the subcellular localization of P450arom (E2 synthase). P450arom immunoreactivity was observed in granule cells at synapses (Fig. 4B), suggesting that E2 can be synthesized within a synapse and that E2 can modulate spinogenesis via synaptic ERα. Preadsorption of the antibody with ERα antigen or P450arom antigen (30 μg/ml each) resulted in the disappearance of immunoreactivity.

Discussion

The current study has demonstrated that the activation of ER by E2 induces a rapid increase of spines on granule neurons in the adult male hippocampal DG region. There is evidence that the perforant path originating in the entorhinal cortex provides excitatory inputs to DG neurons via granule cell dendrites in the molecular layer (Thomas et al., 1994; Dolorfo and Amaral, 1998). The current results imply that E2 may significantly enhance the excitatory input to DG by increasing the density of spines.

Kinase-mediated signaling model for rapid effect of E2 on spinogenesis

The current results regarding kinase inhibition suggest that the rapid effects of E2 are mediated by serine/threonine kinases, including Erk MAPK, PKA, and PKC (Fig. 5). Because both ER and these kinases are present in spines, an efficient coupling between these proteins could occur postsynaptically (Milner et al., 2005; Mukai et al., 2007; Hojo

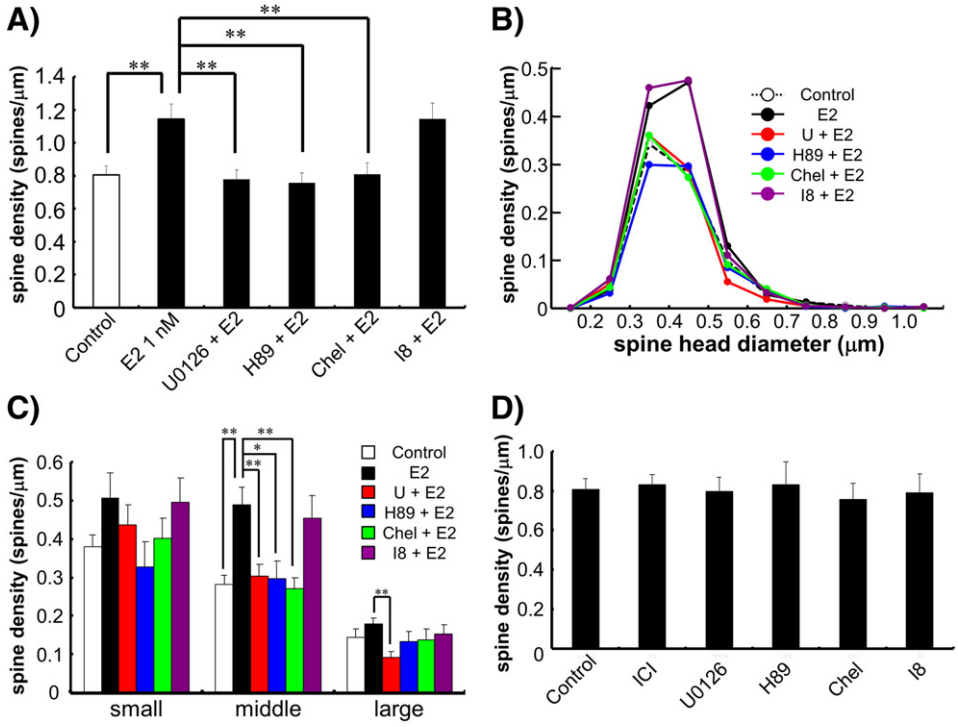

Fig. 3. Effects of kinase blockers on E2-induced spine increase and change in morphology. (A) Effect of kinase inhibitors in the presence of E2 on the total spine density in DG neurons. A 2-h treatment in ACSF without E2 (control), with 1 nM E2, 1 nM E2 and 25 μM U0126 (U; Erk MAPK inhibitor), 1 nM E2 and 10 μM H-89 (H89; PKA inhibitor), 1 nM E2 and 10 μM Chelerythrine (Chel; PKC inhibitor), and 1 nM E2 and 50 μM Inhibitor 8 (I8; GSK-3β inhibitor). (B) Histogram of spine head diameters after a 2-h treatment in ACSF without E2 (control, open circle and dashed line), with 1 nM E2 (black line), E2 and U (red line), E2 and H89 (blue line), E2 and Chel (green line), and E2 and I8 (purple line). (C) Density of 3 subtypes of spines. Abbreviations are same as in (B). From left to right, small-head spines (small), middle-head spines (middle), and large-head spines (large). In each group, control (open column), E2 (black column), E2 + U0126 (red column), E2 + H89 (blue column), E2 + Chel (green column), and E2 + I8 (purple column). (D) No effects by blockers only. Vertical axis is the average number of spines per 1 μm of dendrite. Results are reported as the mean ± SEM. Significance is defined as *: $P < 0.05$, **: $P < 0.01$ versus control or 1 nM E2. In (A)–(D), data are represented as the mean ± SEM. Statistical significance is defined as *$P < 0.05$, **$P < 0.01$ vs E2 sample. For each drug treatment, we investigated 3 rats, 7 slices, 14 neurons, 28 dendrites and 1400–2000 spines. For the control, we used 5 rats, 8 slices, 16 neurons, 31 dendrites and approx. 1700 spines.

et al., 2008). MAPK, PKA, and PKC are involved in rapid E2 signaling not only in DG but also in CA1 and CA3 (Tsurugizawa et al., 2005; Mukai et al., 2006a, 2006b, 2010; Murakami et al., 2006b; Hasegawa et al., 2015). Rapid phosphorylation of MAPK and PKA by E2 has been demonstrated in earlier works of hippocampus (Kim et al., 2002; Toran-Allerand et al., 2002; Lee et al., 2004).

As an example, in the CA1 region, a MAPK cascade for E2 signaling has been suggested, which couples with PKA and PKC through PKC → Raf1 → MAPK, PKA → B-Raf → MAPK in synaptic modulation, according to an LTP study (Roberson et al., 1999). In DG, PKA, PKC and MAPK could be coupled in the same manner as in CA1. Erk MAPK is known to phosphorylate cortactin, a structural protein associated with actin (MacQueen et al., 2003). Cortactin interacts with both F-actin and actin-related protein (Arp) 2/3 complexes, as well as the scaffold protein Shank in the PSD at the SH3 domain (Weed et al., 1998; Campbell et al., 1999), resulting in the promotion of actin fiber remodeling within spines. As an example, upon BDNF stimulation, MAPK phosphorylates cortactin through interaction with the C-terminal of the SH3 domain, resulting in a reorganization of spine morphology (Iki et al., 2005). It is thus possible that E2 exerts its effect on spines through a cortactin-actin pathway. Cortactin has multiple phosphorylation sites, including Ser^{405} and Ser^{418}, that are activated by MAPK (Campbell et al., 1999). Phosphorylation of cortactin may promote assembly of actin cytoskeletal matrices, resulting in spine formation or

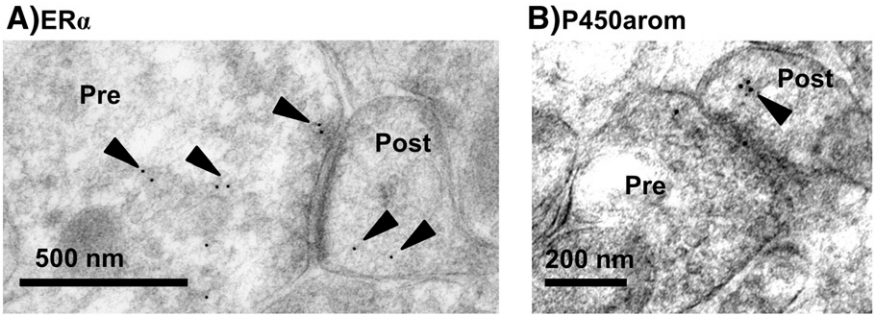

Fig. 4. Immunoelectron microscopic analysis of the distribution of ERα (A) and P450arom (B) within the axospinous synapses onto granule neurons in the outer molecular layer of DG. Representative pictures are shown from approx. 100 photographs, taken of 25 independent slices from five animals. Gold particles (arrowheads) were localized in the pre- and post-synaptic regions. pre, presynaptic region; post, postsynaptic region. A 1/1000 dilution for RC-19 and a 1/500 dilution for P450arom IgG were used to prevent nonspecific labeling. Scale bar: 500 nm for panel A and 200 nm for panel B.

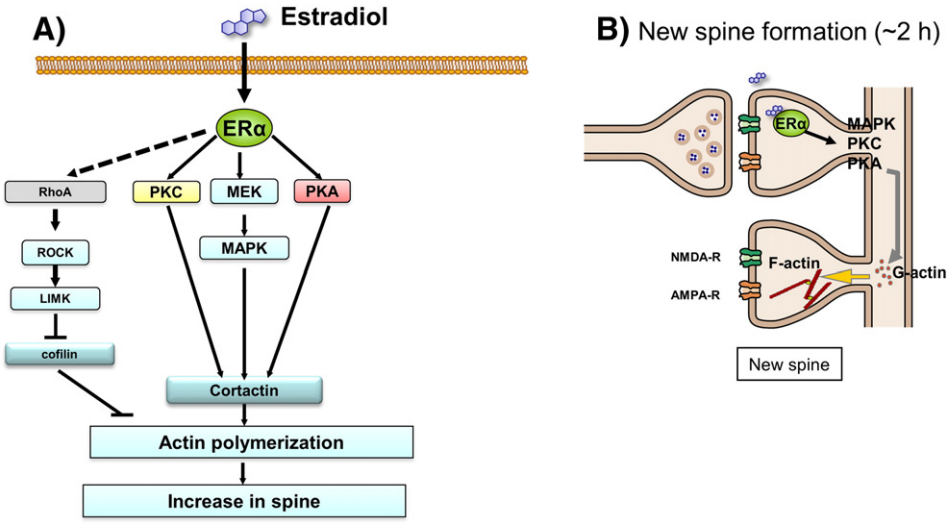

Fig. 5. Hypothetical model illustration for E2-induced spine formation in DG through kinase networks.

modulation of spine heads (Hering and Sheng, 2003). These and other sites, including Ser^{113}, are also putative phosphorylation sites for other serine/threonine kinases (i.e., PKA or PKC) that are activated by E2.

In addition to cortactin, cofilin and LIMK are also good candidates for mediators of E2-induced actin reassembly leading to spinogenesis (Aizawa et al., 2001; Liston et al., 2013; Hasegawa et al., 2015). It is known that E2 induces the phosphorylation of both LIMK and cofilin, leading to actin filament modulation (Yuen et al., 2011). LIMK phosphorylates cofilin, resulting in assembly of actin cytoskeletal matrices (Bernstein and Bamburg; Yang et al., 1998; Yuen et al., 2011). PKC or RhoA may phosphorylate LIMK (Pilpel and Segal, 2004; Shi et al., 2009). GSK-3β, however, was found to be uninvolved in E2 signaling of DG spinogenesis, even though it participates in E2 signaling of CA1 spinogenesis (Hasegawa et al., 2015).

Interestingly, the effect of E2 was completely blocked by inhibition of single kinases (MAPK, PKA, PKC or LIMK), although several kinases participate in E2-induced spinogenesis (Fig. 3). These results suggest that E2-induced increases in spine density may require multiple phosphorylation of actin-modulating proteins, including cortactin and cofilin, to proceed.

DG functions and effects of sex hormones

Neurogenesis and synaptic plasticity, including LTP, have been extensively studied in DG (Clelland et al., 2009; Lisman, 2011; Nakashiba et al., 2012). Chronic effects of sex hormones on DG functions have also been investigated. Mild exercise increases levels of hippocampus-synthesized dihydrotestosterone, resulting in the enhancement of neurogenesis (Okamoto et al., 2012). E2 chronically increases neurogenesis (Ormerod et al., 2003; Perez-Martin et al., 2003a, 2003b; Isgor and Watson, 2005). The chronic increase in spine density by E2 has also been studied. E2 was shown to have no effect on the spine density in DG granule cells upon daily injection of E2 into ovariectomy (OVX) animals for 3 days, although the same pattern of E2 injections significantly increased the spine density in CA1 (Gould et al., 1990). Golgi staining of spines was used for these evaluations (Gould et al., 1990), but this method might not produce images with high enough resolution to discern DG spine changes. Therefore, we used Lucifer Yellow staining of single neurons in combination with 3D image analysis by Spiso-3D to improve the resolution. These methods allowed us to successfully observe E2-induced changes in the spine density and morphology (Fig. 1). Camera lucida imaging of Golgi staining shows only 2-dimensional images (=projection of 3-D optical slice images onto 2-D plane) where several spines may overlap one another. Whereas the current study uses the whole 3-D stack images for Spiso-3D analysis which is devoid of miss-counting of overlapped spines on 2-D image projection. In addition, Golgi methods stain dendrites of many neurons, may be leading to a trouble of miss-counting of dendritic spines from different neurons. On the other hand, single neuron Lucifer Yellow injection stains dendrites of only one neuron.

Involvement of PKA in chronic spinogenesis upon E2 treatment has also been demonstrated in primary cultured hippocampal neurons (Murphy and Segal, 1996; Segal and Murphy, 1998).

As one of a few examples for rapid effects of E2, 20 min application of letrozole, a P450arom inhibitor, suppressed LTP in the perforant pathway, and co-application of 4 nM E2 with letrozole rescued LTP (Tanaka and Sokabe, 2012), suggesting that hippocampus-synthesized E2 (rapid synthesis) is essential for LTP induction in DG. The current study may be the first demonstration of the rapid effects of E2 on spinogenesis in DG.

The total spine density of DG granule cells (0.81 spines/μm) was significantly smaller than that of CA1 pyramidal neurons (approx. 1.0 spines/μm) (Mukai et al., 2011; Hasegawa et al., 2015). In both DG and CA1, incubation with 1 nM E2 increased the spine density by approx. 140–150% after 2 h incubation. On the other hand, in CA3 pyramidal neurons, the total density of thorns (spine-like postsynaptic structures that are found in CA3 stratum lucidum), which contact mossy fiber terminals originating from granule cells, decreased to approx. 70% upon treatment (Tsurugizawa et al., 2005). Estradiol-induced spinogenesis is thus highly region-specific and heterogeneous.

We observed E2-concentration-dependent enlargement of spine heads on hippocampal DG neurons. By changing the incubation concentrations from 1 nM to 10 nM E2, the density of large-head spines was increased (Fig. 2). Because the density of AMPA receptors is significantly greater in large-head spines than in small-head spines (Shinohara et al., 2008), 10 nM E2 may enhance memory-related synaptic activity more than 1 nM E2 may do. From mass spectrometric analysis of freshly isolated hippocampus, E2 levels varied between 2 and 13 nM, with an average level of approx. 8 nM (Hojo et al., 2009). E2 concentrations of 1 nM and 10 nM are thus within the physiological range of E2 levels. Note that during the step in which hippocampal slices are incubated in ACSF to obtain the 'acute' isolated slices, normally used for analysis of synaptic plasticity, levels of E2 decreased to below 0.5 nM due to E2 leakage (Hojo et al., 2009, 2011). Accordingly, the increase in spine density observed upon application of 1 nM or 10 nM E2 in the current study may be a rescue-related effect. We should also note that all E2 is free (i.e., active) in neurons, because in neurons no E2 binding proteins are present.

Because the rapid effects of E2 on spinogenesis were blocked by the ER antagonist ICI, these effects are likely mediated by synaptic ER. Interestingly, both ERα and P450arom were expressed in the spines of granule neurons (Fig. 4), suggesting that spine-produced E2 could rapidly modulate spinogenesis via synaptic ERα (synaptocrinology). Although the E2-induced spinogenesis was mediated by postsynaptic ERα, presynaptic ERα (Fig. 4) may potentiate excitatory synaptic transmission as observed in CA1 pyramidal neurons (Smejkalova and Woolley, 2010).

E2 responsiveness of granule cell spines may be complex. Female DG granule spines have a poor response to estrus cycle (Gould et al., 1990; Miranda et al., 1999; Woolley et al., 1990). Miranda et al. (1999) used Camera lucida imaging of Lucifer Yellow-filled neurons, and demonstrated that the DG spine density of young and aged OVX female increased upon short E2 exposure (E2 injection and waiting 24–48 h), however, the spine density did not respond to long term E2 exposure (> several months). In their conditions, young OVX female was deprived of E2 for relatively short period and aged OVX female was deprived of E2 for long period. In the current experiments, we used young male rat slices (2 h-short deprivation of E2 by recovery incubation in ACSF) with very short term E2 exposure (2 h). From these considerations, a high E2-responsiveness may be induced by short E2 exposure to E2-depleted DG neurons. Miranda et al. (1999) did not find a change in spine density in vivo by 10 μg E2 injection to castrated males (Miranda et al., 1999). These results may be due to the fact that castration did not decrease the male hippocampal high E2 level (~8 nM) (Hojo et al., 2009). On the other hand, in female rats OVX decreased hippocampal E2 level to ~0.7 nM (Kato et al., 2013). Therefore, in order to obtain male spine increase by E2 injection, we might need to inject much more than 10 μg E2 which Miranda et al. (1999) used. Injection of 10 μg E2 is strong enough for the female hippocampus but may be too weak for the male hippocampus.

Acknowledgments

We thank Prof. John H. Morrison (Mount Sinai School of Medicine) for immunoelectron microscopic analysis.

References

Adams, M.M., Fink, S.E., Shah, R.A., Janssen, W.G., Hayashi, S., Milner, T.A., McEwen, B.S., Morrison, J.H., 2002. Estrogen and aging affect the subcellular distribution of estrogen receptor-alpha in the hippocampus of female rats. J. Neurosci. 22, 3608–3614.

Aimone, J.B., Deng, W., Gage, F.H., 2011. Resolving new memories: a critical look at the dentate gyrus, adult neurogenesis, and pattern separation. Neuron 70, 589–596.

Aizawa, H., Wakatsuki, S., Ishii, A., Moriyama, K., Sasaki, Y., Ohashi, K., Sekine-Aizawa, Y., Sehara-Fujisawa, A., Mizuno, K., Goshima, Y., Yahara, I., 2001. Phosphorylation of cofilin by LIM-kinase is necessary for semaphorin 3A-induced growth cone collapse. Nat. Neurosci. 4, 367–373.

Bernstein BW, Bamburg JR ADF/cofilin: a functional node in cell biology. Trends Cell Biol 20:187–195.

Campbell, D.H., Sutherland, R.L., Daly, R.J., 1999. Signaling pathways and structural domains required for phosphorylation of EMS1/cortactin. Cancer Res. 59, 5376–5385.

Clelland, C.D., Choi, M., Romberg, C., Clemenson Jr., G.D., Fragniere, A., Tyers, P., Jessberger, S., Saksida, L.M., Barker, R.A., Gage, F.H., Bussey, T.J., 2009. A functional role for adult hippocampal neurogenesis in spatial pattern separation. Science 325, 210–213.

Dolorfo, C.L., Amaral, D.G., 1998. Entorhinal cortex of the rat: topographic organization of the cells of origin of the perforant path projection to the dentate gyrus. J. Comp. Neurol. 398, 25–48.

Duan, H., Wearne, S.L., Rocher, A.B., Macedo, A., Morrison, J.H., Hof, P.R., 2003. Age-related dendritic and spine changes in corticocortically projecting neurons in macaque monkeys. Cereb. Cortex 13, 950–961.

Gould, E., Woolley, C.S., Frankfurt, M., McEwen, B.S., 1990. Gonadal steroids regulate dendritic spine density in hippocampal pyramidal cells in adulthood. J. Neurosci. 10, 1286–1291.

Hasegawa, Y., Hojo, Y., Kojima, H., Ikeda, M., Hotta, K., Sato, R., Ooishi, Y., Yoshiya, M., Chung, B.C., Yamazaki, T., Kawato, S., 2015. Estradiol rapidly modulates synaptic plasticity of hippocampal neurons: involvement of kinase networks. Brain Res. http://dx.doi.org/10.1016/j.brainres.2014.12.056 (Epub ahead of print).

Hering, H., Sheng, M., 2003. Activity-dependent redistribution and essential role of cortactin in dendritic spine morphogenesis. J. Neurosci. 23, 11759–11769.

Hojo, Y., Hattori, T.A., Enami, T., Furukawa, A., Suzuki, K., Ishii, H.T., Mukai, H., Morrison, J.H., Janssen, W.G., Kominami, S., Harada, N., Kimoto, T., Kawato, S., 2004. Adult male rat hippocampus synthesizes estradiol from pregnenolone by cytochromes P45017alpha and P450 aromatase localized in neurons. Proc. Natl. Acad. Sci. U. S. A. 101, 865–870.

Hojo, Y., Murakami, G., Mukai, H., Higo, S., Hatanaka, Y., Ogiue-Ikeda, M., Ishii, H., Kimoto, T., Kawato, S., 2008. Estrogen synthesis in the brain—role in synaptic plasticity and memory. Mol. Cell. Endocrinol. 290, 31–43.

Hojo, Y., Higo, S., Ishii, H., Ooishi, Y., Mukai, H., Murakami, G., Kominami, T., Kimoto, T., Honma, S., Poirier, D., Kawato, S., 2009. Comparison between hippocampus-synthesized and circulation-derived sex steroids in the hippocampus. Endocrinology 150, 5106–5112.

Hojo, Y., Higo, S., Kawato, S., Hatanaka, Y., Ooishi, Y., Murakami, G., Ishii, H., Komatsuzaki, Y., Ogiue-Ikeda, M., Mukai, H., Kimoto, T., 2011. Hippocampal synthesis of sex steroids and corticosteroids: essential for modulation of synaptic plasticity. Front. Endocrinol. 2, 43 (Lausanne).

Hojo, Y., Okamoto, M., Kato, A., Higo, S., Sakai, F., Soya, H., Yamazaki, T., Kawato, S., 2014. Neurosteroid synthesis in adult female rat hippocampus, including androgens and allopregnanolone. J. Steroids Hormonal Sci. Article S4.

Iki, J., Inoue, A., Bito, H., Okabe, S., 2005. Bi-directional regulation of postsynaptic cortactin distribution by BDNF and NMDA receptor activity. Eur. J. Neurosci. 22, 2985–2994.

Isgor, C., Watson, S.J., 2005. Estrogen receptor alpha and beta mRNA expressions by proliferating and differentiating cells in the adult rat dentate gyrus and subventricular zone. Neuroscience 134, 847–856.

Ishii, H., Tsurugizawa, T., Ogiue-Ikeda, M., Asashima, M., Mukai, H., Murakami, G., Hojo, Y., Kimoto, T., Kawato, S., 2007. Local production of sex hormones and their modulation of hippocampal synaptic plasticity. Neuroscientist 13, 323–334.

Kato, A., Hojo, Y., Higo, S., Komatsuzaki, Y., Murakami, G., Yoshino, H., Uebayashi, M., Kawato, S., 2013. Female hippocampal estrogens have a significant correlation with cyclic fluctuation of hippocampal spines. Front. Neural Circuits 7, 149.

Kawato, S., Hojo, Y., Kimoto, T., 2002. Histological and metabolism analysis of P450 expression in the brain. Methods Enzymol. 357, 241–249.

Kawato, S., Yamada, M., Kimoto, T., 2003. Brain neurosteroids are 4th generation neuromessengers in the brain: cell biophysical analysis of steroid signal transduction. Adv. Biophys. 37, 1–48.

Kim, J.S., Kim, H.Y., Kim, J.H., Shin, H.K., Lee, S.H., Lee, Y.S., Son, H., 2002. Enhancement of rat hippocampal long-term potentiation by 17 beta-estradiol involves mitogen-activated protein kinase-dependent and -independent components. Neurosci. Lett. 332, 65–69.

Kimoto, T., Tsurugizawa, T., Ohta, Y., Makino, J., Tamura, H., Hojo, Y., Takata, N., Kawato, S., 2001. Neurosteroid synthesis by cytochrome p450-containing systems localized in the rat brain hippocampal neurons: N-methyl-D-aspartate and calcium-dependent synthesis. Endocrinology 142, 3578–3589.

Kretz, O., Fester, L., Wehrenberg, U., Zhou, L., Brauckmann, S., Zhao, S., Prange-Kiel, J., Naumann, T., Jarry, H., Frotscher, M., Rune, G.M., 2004. Hippocampal synapses depend on hippocampal estrogen synthesis. J. Neurosci. 24, 5913–5921.

Kuiper, G.G., Carlsson, B., Grandien, K., Enmark, E., Haggblad, J., Nilsson, S., Gustafsson, J.A., 1997. Comparison of the ligand binding specificity and transcript tissue distribution of estrogen receptors alpha and beta. Endocrinology 138, 863–870.

Lee, S.J., Campomanes, C.R., Sikat, P.T., Greenfield, A.T., Allen, P.B., McEwen, B.S., 2004. Estrogen induces phosphorylation of cyclic AMP response element binding (pCREB) in primary hippocampal cells in a time-dependent manner. Neuroscience 124, 549–560.

Leranth, C., Petnehazy, O., MacLusky, N.J., 2003. Gonadal hormones affect spine synaptic density in the CA1 hippocampal subfield of male rats. J. Neurosci. 23, 1588–1592.

Lisman, J., 2011. Formation of the non-functional and functional pools of granule cells in the dentate gyrus: role of neurogenesis, LTP and LTD. J. Physiol. 589, 1905–1909.

Liston, C., Cichon, J.M., Jeanneteau, F., Jia, Z., Chao, M.V., Gan, W.B., 2013. Circadian glucocorticoid oscillations promote learning-dependent synapse formation and maintenance. Nat. Neurosci. 16, 698–705.

Liu, X., Ramirez, S., Tonegawa, S., 2014. Inception of a false memory by optogenetic manipulation of a hippocampal memory engram. Philos. Trans. R. Soc. Lond. Ser. B Biol. Sci. 369, 20130142.

Luine, V.N., 2014. Estradiol and cognitive function: past, present and future. Horm. Behav. 66, 602–618.

MacQueen, G.M., Campbell, S., McEwen, B.S., Macdonald, K., Amano, S., Joffe, R.T., Nahmias, C., Young, L.T., 2003. Course of illness, hippocampal function, and hippocampal volume in major depression. Proc. Natl. Acad. Sci. U. S. A. 100, 1387–1392.

McHugh, T.J., Jones, M.W., Quinn, J.J., Balthasar, N., Coppari, R., Elmquist, J.K., Lowell, B.B., Fanselow, M.S., Wilson, M.A., Tonegawa, S., 2007. Dentate gyrus NMDA receptors mediate rapid pattern separation in the hippocampal network. Science 317, 94–99.

Milner, T.A., Ayoola, K., Drake, C.T., Herrick, S.P., Tabori, N.E., McEwen, B.S., Warrier, S., Alves, S.E., 2005. Ultrastructural localization of estrogen receptor beta immunoreactivity in the rat hippocampal formation. J. Comp. Neurol. 491, 81–95.

Miranda, P., Williams, C.L., Einstein, G., 1999. Granule cells in aging rats are sexually dimorphic in their response to estradiol. J. Neurosci. 19, 3316–3325.

Mukai, H., Takata, N., Ishii, H.T., Tanabe, N., Hojo, Y., Furukawa, A., Kimoto, T., Kawato, S., 2006a. Hippocampal synthesis of estrogens and androgens which are paracrine modulators of synaptic plasticity: synaptocrinology. Neuroscience 138, 757–764.

Mukai, H., Tsurugizawa, T., Ogiue-Ikeda, M., Murakami, G., Hojo, Y., Ishii, H., Kimoto, T., Kawato, S., 2006b. Local neurosteroid production in the hippocampus: influence on synaptic plasticity of memory. Neuroendocrinology 84, 255–263.

Mukai, H., Tsurugizawa, T., Murakami, G., Kominami, S., Ishii, H., Ogiue-Ikeda, M., Takata, N., Tanabe, N., Furukawa, A., Hojo, Y., Ooishi, Y., Morrison, J.H., Janssen, W.G., Rose, J.A., Chambon, P., Kato, S., Izumi, S., Yamazaki, T., Kimoto, T., Kawato, S., 2007. Rapid modulation of long-term depression and spinogenesis via synaptic estrogen receptors in hippocampal principal neurons. J. Neurochem. 100, 950–967.

Mukai, H., Kimoto, T., Hojo, Y., Kawato, S., Murakami, G., Higo, S., Hatanaka, Y., Ogiue-Ikeda, M., 2010. Modulation of synaptic plasticity by brain estrogen in the hippocampus. Biochim. Biophys. Acta 1800, 1030–1044.

Mukai, H., Hatanaka, Y., Mitsuhashi, K., Hojo, Y., Komatsuzaki, Y., Sato, R., Murakami, G., Kimoto, T., Kawato, S., 2011. Automated analysis of spines from confocal laser microscopy images: application to the discrimination of androgen and estrogen effects on spinogenesis. Cereb. Cortex 21, 2704–2711.

Munetsuna, E., Hojo, Y., Hattori, M., Ishii, H., Kawato, S., Ishida, A., Kominami, S.A., Yamazaki, T., 2009. Retinoic acid stimulates 17beta-estradiol and testosterone synthesis in rat hippocampal slice cultures. Endocrinology 150, 4260–4269.

Murakami, G., Tanabe, N., Ishii, H.T., Ogiue-Ikeda, M., Tsurugizawa, T., Mukai, H., Hojo, Y., Takata, N., Furukawa, A., Kimoto, T., Kawato, S., 2006a. Role of cytochrome p450 in synaptocrinology: endogenous estrogen synthesis in the brain hippocampus. Drug Metab. Rev. 38, 353–369.

Murakami, G., Tsurugizawa, T., Hatanaka, Y., Komatsuzaki, Y., Tanabe, N., Mukai, H., Hojo, Y., Kominami, S., Yamazaki, T., Kimoto, T., Kawato, S., 2006b. Comparison between basal and apical dendritic spines in estrogen-induced rapid spinogenesis of CA1 principal neurons in the adult hippocampus. Biochem. Biophys. Res. Commun. 351, 553–558.

Murakami, G., Hojo, Y., Ogiue-Ikeda, M., Mukai, H., Chambon, P., Nakajima, K., Ooishi, Y., Kimoto, T., Kawato, S., 2014. Estrogen receptor KO mice study on rapid modulation of spines and long-term depression in the hippocampus. Brain Res. http://dx.doi.org/10.1016/j.brainres.2014.12.002 (Epub ahead of print).

Murphy, D.D., Segal, M., 1996. Regulation of dendritic spine density in cultured rat hippocampal neurons by steroid hormones. J. Neurosci. 16, 4059–4068.

Nakashiba, T., Cushman, J.D., Pelkey, K.A., Renaudineau, S., Buhl, D.L., McHugh, T.J., Rodriguez Barrera, V., Chittajallu, R., Iwamoto, K.S., McBain, C.J., Fanselow, M.S., Tonegawa, S., 2012. Young dentate granule cells mediate pattern separation, whereas old granule cells facilitate pattern completion. Cell 149, 188–201.

Ogiue-Ikeda, M., Tanabe, N., Mukai, H., Hojo, Y., Murakami, G., Tsurugizawa, T., Takata, N., Kimoto, T., Kawato, S., 2008. Rapid modulation of synaptic plasticity by estrogens as well as endocrine disrupters in hippocampal neurons. Brain Res. Rev. 57, 363–375.

Okamoto, M., Hojo, Y., Inoue, K., Matsui, T., Kawato, S., McEwen, B.S., Soya, H., 2012. Mild exercise increases dihydrotestosterone in hippocampus providing evidence for androgenic mediation of neurogenesis. Proc. Natl. Acad. Sci. U. S. A. 109, 13100–13105.

Olariu, A., Cleaver, K.M., Shore, L.E., Brewer, M.D., Cameron, H.A., 2005. A natural form of learning can increase and decrease the survival of new neurons in the dentate gyrus. Hippocampus 15, 750–762.

Ooishi, Y., Kawato, S., Hojo, Y., Hatanaka, Y., Higo, S., Murakami, G., Komatsuzaki, Y., Ogiue-Ikeda, M., Kimoto, T., Mukai, H., 2012a. Modulation of synaptic plasticity in the hippocampus by hippocampus-derived estrogen and androgen. J. Steroid Biochem. Mol. Biol. 131, 37–51.

Ooishi, Y., Mukai, H., Hojo, Y., Murakami, G., Hasegawa, Y., Shindo, T., Morrison, J.H., Kimoto, T., Kawato, S., 2012b. Estradiol rapidly rescues synaptic transmission from corticosterone-induced suppression via synaptic/extranuclear steroid receptors in the hippocampus. Cereb. Cortex 22, 926–936.

Ormerod, B.K., Lee, T.T., Galea, L.A., 2003. Estradiol initially enhances but subsequently suppresses (via adrenal steroids) granule cell proliferation in the dentate gyrus of adult female rats. J. Neurobiol. 55, 247–260.

Perez-Martin, M., Azcoitia, I., Trejo, J.L., Sierra, A., Garcia-Segura, L.M., 2003a. An antagonist of estrogen receptors blocks the induction of adult neurogenesis by insulin-like growth factor-I in the dentate gyrus of adult female rat. Eur. J. Neurosci. 18, 923–930.

Perez-Martin, M., Cifuentes, M., Grondona, J.M., Bermudez-Silva, F.J., Arrabal, P.M., Perez-Figares, J.M., Jimenez, A.J., Garcia-Segura, L.M., Fernandez-Llebrez, P., Fernandez-Llebrez, P., 2003b. Neurogenesis in explants from the walls of the lateral ventricle of adult bovine brain: role of endogenous IGF-1 as a survival factor. Eur. J. Neurosci. 17, 205–211.

Pettorossi, V.E., Di Mauro, M., Scarduzio, M., Panichi, R., Tozzi, A., Calabresi, P., Grassi, S., 2013. Modulatory role of androgenic and estrogenic neurosteroids in determining the direction of synaptic plasticity in the CA1 hippocampal region of male rats. Physiol. Rep. 1, e00185.

Pilpel, Y., Segal, M., 2004. Activation of PKC induces rapid morphological plasticity in dendrites of hippocampal neurons via Rac and Rho-dependent mechanisms. Eur. J. Neurosci. 19, 3151–3164.

Roberson, E.D., English, J.D., Adams, J.P., Selcher, J.C., Kondratick, C., Sweatt, J.D., 1999. The mitogen-activated protein kinase cascade couples PKA and PKC to cAMP response element binding protein phosphorylation in area CA1 of hippocampus. J. Neurosci. 19, 4337–4348.

Segal, M., Murphy, D.D., 1998. CREB activation mediates plasticity in cultured hippocampal neurons. Neural Plast. 6, 1–7.

Shi, Y., Pontrello, C.G., DeFea, K.A., Reichardt, L.F., Ethell, I.M., 2009. Focal adhesion kinase acts downstream of EphB receptors to maintain mature dendritic spines by regulating cofilin activity. J. Neurosci. 29, 8129–8142.

Shinohara, Y., Hirase, H., Watanabe, M., Itakura, M., Takahashi, M., Shigemoto, R., 2008. Left-right asymmetry of the hippocampal synapses with differential subunit allocation of glutamate receptors. Proc. Natl. Acad. Sci. U. S. A. 105, 19498–19503.

Smejkalova, T., Woolley, C.S., 2010. Estradiol acutely potentiates hippocampal excitatory synaptic transmission through a presynaptic mechanism. J. Neurosci. 30, 16137–16148.

Tanaka, M., Sokabe, M., 2012. Continuous de novo synthesis of neurosteroids is required for normal synaptic transmission and plasticity in the dentate gyrus of the rat hippocampus. Neuropharmacology 62, 2373–2387.

Tanapat, P., Hastings, N.B., Gould, E., 2005. Ovarian steroids influence cell proliferation in the dentate gyrus of the adult female rat in a dose- and time-dependent manner. J. Comp. Neurol. 481, 252–265.

Thomas, K.L., Laroche, S., Errington, M.L., Bliss, T.V., Hunt, S.P., 1994. Spatial and temporal changes in signal transduction pathways during LTP. Neuron 13, 737–745.

Toran-Allerand, C.D., Guan, X., MacLusky, N.J., Horvath, T.L., Diano, S., Singh, M., Connolly Jr., E.S., Nethrapalli, I.S., Tinnikov, A.A., 2002. ER-X: a novel, plasma membrane-associated, putative estrogen receptor that is regulated during development and after ischemic brain injury. J. Neurosci. 22, 8391–8401.

Trommald, M., Hulleberg, G., Andersen, P., 1996. Long-term potentiation is associated with new excitatory spine synapses on rat dentate granule cells. Learn. Mem. 3, 218–228.

Tsurugizawa, T., Mukai, H., Tanabe, N., Murakami, G., Hojo, Y., Kominami, S., Mitsuhashi, K., Komatsuzaki, Y., Morrison, J.H., Janssen, W.G., Kimoto, T., Kawato, S., 2005. Estrogen induces rapid decrease in dendritic thorns of CA3 pyramidal neurons in adult male rat hippocampus. Biochem. Biophys. Res. Commun. 337, 1345–1352.

Weed, S.A., Du, Y., Parsons, J.T., 1998. Translocation of cortactin to the cell periphery is mediated by the small GTPase Rac1. J. Cell Sci. 111 (Pt 16), 2433–2443.

Woolley, C.S., McEwen, B.S., 1992. Estradiol mediates fluctuation in hippocampal synapse density during the estrous cycle in the adult rat. J. Neurosci. 12, 2549–2554.

Woolley, C.S., Gould, E., Frankfurt, M., McEwen, B.S., 1990. Naturally occurring fluctuation in dendritic spine density on adult hippocampal pyramidal neurons. J. Neurosci. 10, 4035–4039.

Yang, N., Higuchi, O., Ohashi, K., Nagata, K., Wada, A., Kangawa, K., Nishida, E., Mizuno, K., 1998. Cofilin phosphorylation by LIM-kinase 1 and its role in Rac-mediated actin reorganization. Nature 393, 809–812.

Yuen, G.S., McEwen, B.S., Akama, K.T., 2011. LIM kinase mediates estrogen action on the actin depolymerization factor Cofilin. Brain Res. 1379, 44–52.